substance: boron compounds with group III elements
property: properties of $Al_3C_2B_{48}$, $Al_3B_{48}C_2$, $C_2Al_3B_{48}$, $B_{48}Al_3C_2$

The compounds $B_{44}Al_3C_2$ (tetragonal) [10B], AlB_{12}(intergrown phases 3 $AlB_{12}{\cdot}2B_4C$, P4/nnm or subgroup) [36M], β-AlB_{12} [58K, 60K] (Imma, complexly twinned at (110) and (1 $\bar{1}$ 0)) and $B_{48}Al_3C_2$ [64M, 65M] (phase 1:Cmma or C2ma; phase 2: Ammm, A222 or A2mm) are attributed to the low-temperature phase of this structure. Moreover a high-temperature phase of the composition $B_{48}Al_3C_2$ with space group P4/nmm, P4/n or $P4_2/n$) [64M, 65M] and space group $P4_2/nnm$ respectively [98M] was found. For a detailed discussion and older references, see [98M].

Preparation [79S, 77M], crystalline structure [77M, 70M]

Structure: orthorhombic

Space group: Im2b

Structure in Fig. 1 [98M].

Preparation and structure in [90O, 98M].

Preparation by hot-pressing in [91K1].

$B_{48}Al_3C_2$ – A filled variant of tetragonal boron [95H2].

lattice parameters (low temperature phase)
(in Å)

a	12.390(3)	*T* = 300 K	X-ray diffraction	98M
b	12.637(3)			
c	10.136(4)			

lattice parameters (high temperature phase)

a	8.85 Å	*T* = 300 K	X-ray diffraction	98M
c	5.10 Å			

occupancies of the Al positions (low temperature phase)

Al(1)	0.445(3)	*T* = 300 K	98M
Al(2)A*)	0.314(3)		
Al(2)B*)	0.151(3)		
Al(3)A*)	0.312(2)		
Al(3)B*)	0.169(3)		

*) the sites Al(2) and Al(3) are disordered.

The coordination of Al(1) between the edges of two icosahedra (Fig. 2) causes a dilatation of the bonds between the involved icosahedral B atoms (2.01 Å instead of 1.67...1.94 Å) and reduces the tetragonal symmetry [98M].

Coordination polyhedra of Al(1), Al(2)/Al(3) and C(1/2) atoms in the structure in Fig. 3 [98M].

For positions of the atoms and distances see [98M].

In [95H1] the structure was described as a filled and distorted variant of α-tetragonal boron (tetragonal boron (I)], space group Imma

lattice parameters
(in Å)

a	12.407(3)	*T* = 300 K		95H1
b	12.623(3)			
c	10.1402(14)			
a	12.302(1)	*T* = 300 K	undoped (Si/B = 0)	94K1
b	12.621(1)			
c	10.161(1)			
a	12.291(2)	*T* = 300 K	Si-doped (Si/B = 0.004)	94K1
b	12.620(4)			
c	10.161(1)			

Dependence of unit cell dimensions on Si content (Si/B ratio < 0.07) in [94K1].

atomic distances
(in Å)

B-B	1.81	*T* = 300 K	intra-icosahedra	95H1
B-B	1.71		inter-icosahedral	
B-C	1.67		average distance to four B in different neighbored icosahedra	
Al(1)-B	1.95		short distance to four B cause lattice distortion	
Al(1)-B	2.44		long distance to other four B	
Al(2, 3)-B	2.1...2.4			

The Al(2), Al(3) sites are partly occupied (~75 %), which leads to a variable Al content and to variable cell constants [95H1].

Reversible phase transition at 650 °C (determined by DTA and X-ray [95H1]) into the tetragonal system [65M].

previous structure analysis

The structure consists of two crystallographically related intergrown orthorhombic phases A (space group Cmma or C2ma) and B (space group Ammm, A222 or A2mm). Towards higher temperatures they gradually transform into a homogeneous phase C (space group P4/nmm, P4/n or $P4_2/n$. At 850 K, this reversible phase transformation is complete [87K].

lattice parameters
(in Å)

a	12.34	*T* = 298 K	phase A	87H
b	12.63			
c	5.08			
a	6.17	*T* = 298 K	phase B	
b	12.63			
c	10.16			
a	8.82	*T* = 1143 K	$(B_{12})_4C_2Al_3$	
c	5.09			

(phase A)

a	12.377(2)...12.363(2)	oscillation Weissenberg and	90O
b	12.627(1)...12.616(1)	precession photography	
c	5.079(1)...5.102(1)		
V	793.8(1)...795.8(2) $Å^3$		

(phase B)

a	6.166(2)...6.181(2)	oscillation Weissenberg and	90O
b	12.635(2)...12.622(1)	precession photography	
c	10.156(2)...10.161(1)		
V	791.2(2)...792.7(2) Å^3		

Further structure investigations of both phases with slightly different lattice parameters in [64M, 86P].

optical transition energies
(in eV)

E_1	~ 1.28	T = 300 K	indirect allowed or non-direct	87H
E_2	2.35		indirect allowed or non-direct	
E_3	2.53		indirect allowed or non-direct	
	2.44		gap, if E2, E3 are attributed to phonon abs. and emission resp. ($\hbar q$ = 725 cm^{-1})	

Transition energies (in eV) derived from the spectra A and B in Fig. 4 [99W]:

	A	B		
E_g	0.45		deep level	99W
		0.60	deep level	
	0.78	0.76	deep level	
		0.96	deep level	
	0.97	1.03	indirect allowed or non-direct	
	2.02	1.91	indirect allowed or non-direct	
	2.10		indirect allowed or non-direct	
	2.26		indirect allowed or non-direct	
	2.34		indirect allowed or non-direct	
	2.40	2.38	indirect allowed or non-direct	
	2.45	2.44	indirect allowed or non-direct	
	2.50	2.50	indirect allowed or non-direct	

Optical absorption edge also in [87H].

phonon wavenumbers (pure $B_{48}Al_3C_2$)
(in cm^{-1})

	IR	Raman		
ν/c		1236	T = 300 K	98M
		1216		
		1196		
		1174		
		1147		
		1119		
		1108		
	1058			
	1042			
		1036		
	1027			
		1017		
	982			
		971		
	948			
	933			
	892	893		
	865			
		861		
		849		
	836			
	806			
		791		
	778			
		769		

	756	
737		
725	726	
	697	
689		
	673	
660	660	
615	616	
	592	
589		
	580	
570		
563		
	556	
	531	
515	516	
	503	
	480	
477		
	464	
	449	
437	435	
420		
	400	
393		
379		
	365	
359		
	349	
	334	
316	314	
	294	
285		
278	276	
	264	
	252	
	237	
233		
	227	
214	215	
	201	
179		
	173	
	156	
	114	
111		
105		

phonon wavenumbers (Si-doped $B_{48}Al_3C_2$ = $B_{48}Al_{1.5}Si_{1.5}C_2$)
(in cm^{-1})

	IR	Raman	
v/c		1202	98M
		1181	
		1144	
		1121	
	1053		
	1040	1040	
		1034	
	1022		
		1015	
	956		

	970
947	
933	
891	893
864	
	853
842802	
	791
777	
	771
753	754
726	
	715
	697
686	
	670
660	
	656
	617
614	
	589
	577
567	
	556
552	
	531
	516
512	
	499
474	474
	460
	449
437	435
	400
391	
379	
359	
	348
313	315
	302
283	
	274
234	234
183	
	180
109	

Phonon spectra (IR and Raman) of pure and Si-doped $Al_3C_2B_{48}$ ($Al_{1.5}Si_{1.5}C_2B_{48}$) in Fig. 5 and Fig. 6 [98M]. IR phonon spectra also in [87H, 87W].

activation energies

E_A	0.6...1.2 eV	T = 100...375 K	electrical conductivity	91P,
		T = 200...400 K		87K

electrical conductivity

(in $\Omega^{-1}cm^{-1}$)

σ	$3.8 \cdot 10^{-2}$ ...	T = 293 K		91P,
	$1 \cdot 10^{-4}$			87K
	$3\ 10^{-2}$	T = 333 K		91K1
	1.1	T = 300 K	Si-doped	94K1

Temperature dependence of the electrical conductivity in Fig. 7 [91K2].

thermoelectric power

S	120 μV K^{-1}	T = 600 K		91K2
	320 μV K^{-1}	T = 1000 K		

Temperature dependence of the Seebeck effect in Fig. 8 [91K2].

Effect of Fe impurities on the thermoelectric power S in Fig. 9 [91K2]

Effect of porosity on σ and S in [91K2]

thermal properties

DTA curves between 615 and 685 °C in Fig. 10 [98M].

microhardness

H_V	2570...3050 kgf/mm^2	T = 300 K		90O
H_K	2060...2300 kgf/mm^2			
H_K	27.1(5) GPa			91K1
H_V	33.6(16) GPa			87K
H	24.51/26.80 GPa		hardness not specified	88B

Microhardness of Si-doped $Al_3C_2B_{48}$ ($Al_{1.5}Si_{1.5}C_2B_{48}$) depending on Si content in Fig. 11 [94K1].

density

d	2.59(2) g cm^{-3}	T = 300 K	floatation method	90O
	2.600 g cm^{-3}			64M

microstrength

σ	1.6/1.8 GPa			88B

microbrittleness

γ	9.3/8.4			88B

fracture toughness

K_c	4(1) $MNm^{-3/2}$			91K1, 87K

References:

10B Biltz, H.: Ber. Dtsch. Chem. Ges. 43 (1910) 297.

36M Mott, N., Jones, H.: The Theory of Properties of Metals and Alloys, 1936, p. 245.

58K Kohn, J.A., Katz, G., Giardini, A.A.: Z. Kristallogr. 111 (1958) 53.

60K Kohn, J.A, Eckard, D.W: Anal. Chem. 32 (1960) 296.

64M Matkovich, V.I., Economy, J., Gieses Jr., R.F.: J. Am. Chem. Soc. 86 (1964) 2337.

65M Matkovich, V.I., Giese, R.F.: Z. Kristallogr. 122 (1965) 108.

70E Economy, J., Matkovich, V. I.: Boron 3, T. Niemyski, ed., PWN Warsaw, 1970 p. 159.

70M Matkovich, V. I., Economy, J.: see [70E] p. 159.

70W Will, G.: see [70E], p. 119.

77B Berezin, A. A., Golikova, O. A., Zaitsev, V. R., Kazanin, M. M., Orlov, V. M., Tkalenko, E. N., in:Boron and Refractory Borides, (Matkovich V. 1., ed.) Springer: Berlin, Heidelberg, New York 1977, p. 52.

77M Matkovich, V. I., Economy, J.: see [77B], p. 96.

77S Spear, K. E.: see [77B1], p. 439.

79S Samsonov, G. V., Neronov, V. A., Lamikhov, L. K.: J. Less-Common Met. 67 (1979) 291.

86P Peshev, P., Gyorov, G., Khristov, M.: J. Less-Common Met. 117 (1986) 341 (Proc. 8th Int. Symp. Boron, Borides, Carbides, Nitrides and Rel. Compounds, Tbilisi, Oct. 8 - 12, 1984).

87H Haupt, H., Werheit, H., Siejak, V., Gurin, V.N., Korsukova, M.M.: in: Proc. 9th Int. Symp. Boron, Borides and Rel. Compounds, University of Duisburg, Germany, Sept. 21 - 25, 1987, H. Werheit ed., University of Duisburg: Duisburg, 1987, p. 387.

87K Kisly, P.S., Prikhna, T.A., Goutar, N.A., Podarevskaya, O.V.: in: Proc. 9th Int. Symp. Boron, Borides and Rel. Compounds, University of Duisburg, Germany, Sept. 21 - 25, 1987, H. Werheit ed., University of Duisburg: Duisburg, 1987, p. 273.

87W Werheit, H.: in: Proc. 9th Int. Symp. Boron, Borides and Rel. Compounds, University of Duisburg, Germany, Sept. 21 - 25, 1987, H. Werheit ed., University of Duisburg: Duisburg, 1987, p. 142.

88B Berdikov, V.F., Vil`k, Yu., Gurin, V.N.: in: Prog. Cryst. Growth Charact. 16 (1988), Gurin, V.N. ed., Pergamon Press: London, 1988, p. 279.

90O Okada, S., Kudou, K., Hiyoshi, H., Higashi, I., Hamano, K., Lundström, T.: J. Ceram Soc. Jpn. Inter. Ed. 98 (1990) 1342.

91K1 Kharlamov, A.I., Loichenko, S.V.: in: Boron-Rich Solids, Proc. 10th Int. Symp. Boron, Borides and Rel. Compounds, Albuquerque, NM 1990 (AIP Conf. Proc. 231), D. Emin, T.L. Aselage, A.C. Switendick, B. Morosin, C.L. Beckel ed., American Institute of Physics: New York, 1991, p. 473.

91K2 Kharlamov, A.I, Loichenko, S.V.: in: Boron-Rich Solids, Proc. 10th Int. Symp. Boron, Borides and Rel. Compounds, Albuquerque, NM 1990 (AIP Conf. Proc. 231), D. Emin, T.L. Aselage, A.C. Switendick, B. Morosin, C.L. Beckel ed., American Institute of Physics: New York, 1991, p. 94.

91P Prikhna, T.A., Kisly, P.S.: in: Boron-Rich Solids, Proc. 10th Int. Symp. Boron, Borides and Rel. Compounds, Albuquerque, NM 1990 (AIP Conf. Proc. 231), D. Emin, T.L. Aselage, A.C. Switendick, B. Morosin, C.L. Beckel ed., American Institute of Physics: New York, 1991, p. 590.

94K1 Kudou, K., Okada, S., Hiyoshi, H., Miyamoto, M., Hikichi, Y., Lundström, T.: J. Soc. Mater. Sci. Jpn. 43 (1994) 223.

94K2 Kumashiro, Y., Yoshizawa, H., Shirai, K.: Proc. 11th Int. Symp. Boron, Borides and Rel. Compounds, Tsukuba, Japan, August 22 - 26, 1993, Jpn. J. Appl. Phys. Series 10 (1994), p. 166.

95H1 Hillebrecht, H., Meyer, F.D.: Z. Kristallogr. Suppl. 10 (1995) 101.

95H2 Hillebrecht, H., Meyer, F.D.: Z. Kristallogr. Suppl. 9 (1995) 176.

98M Meyer, F.D.: in: Thesis, Albert-Ludwigs-Universität Freiburg ed., Freiburg, Germany, 1998 .

99W Werheit, H., Schmechel, R., Meyer, F.D., Hillebrecht, H.: J. Solid State Chem. (2000) (Proc. 13th Int. Symp. Boron, Borides and Rel. Compounds, Dinard, France, Sept. 1999).

Fig. 1.

$Al_3C_2B_{48}$. Crystal structure [98M].

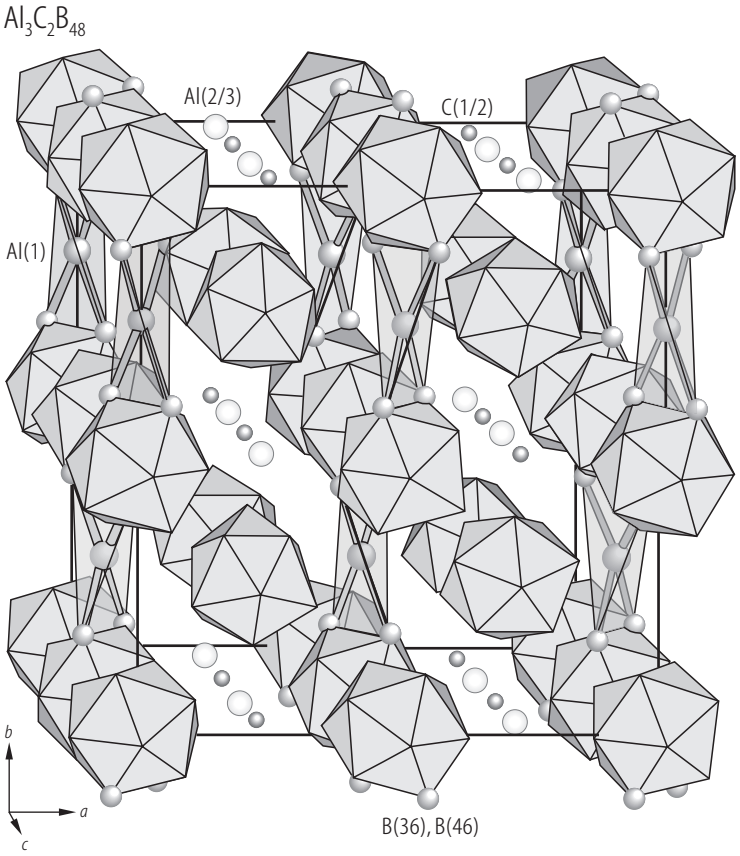

Fig. 2.

$Al_3C_2B_{48}$. Coordination of the Al(1) atom between two icosahedra [98M].

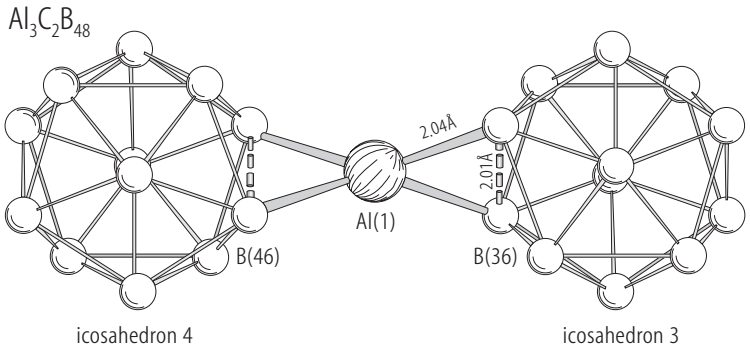

Fig. 3.

$Al_3C_2B_{48}$. Coordination polyhedra of **(a)** Al(1), **(b)** Al(2)/Al(3) and **(c)** C(1/2) atoms in the structure [98M].

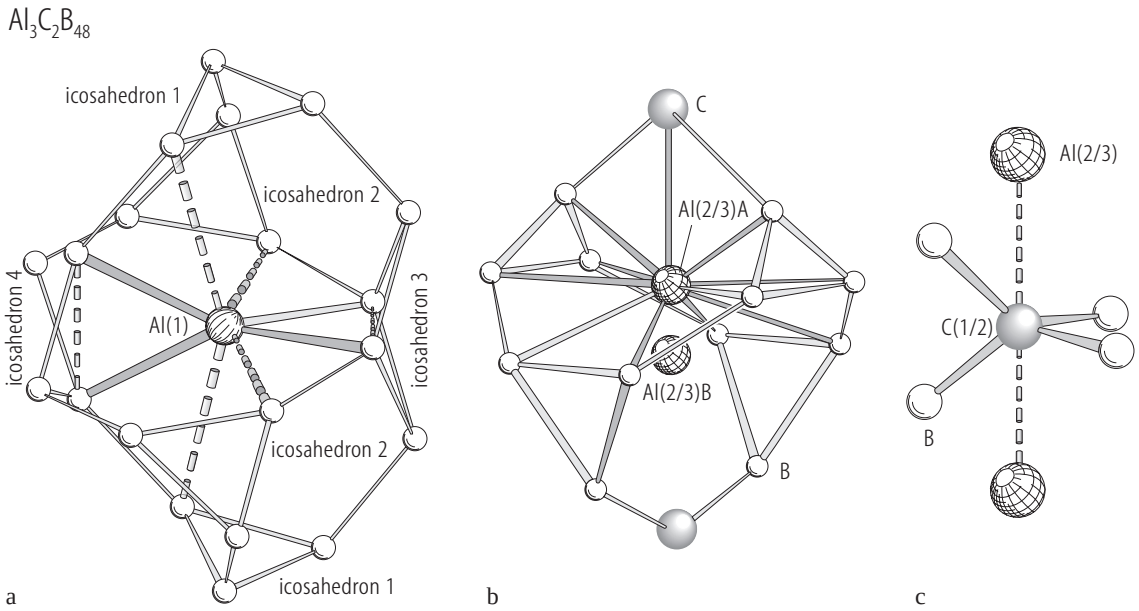

Fig. 4.

$Al_3C_2B_{48}$. Absorption edge; absorption coefficient vs. photon energy. Spectra of two different single crystals of undefined crystallographic orientation [99W].

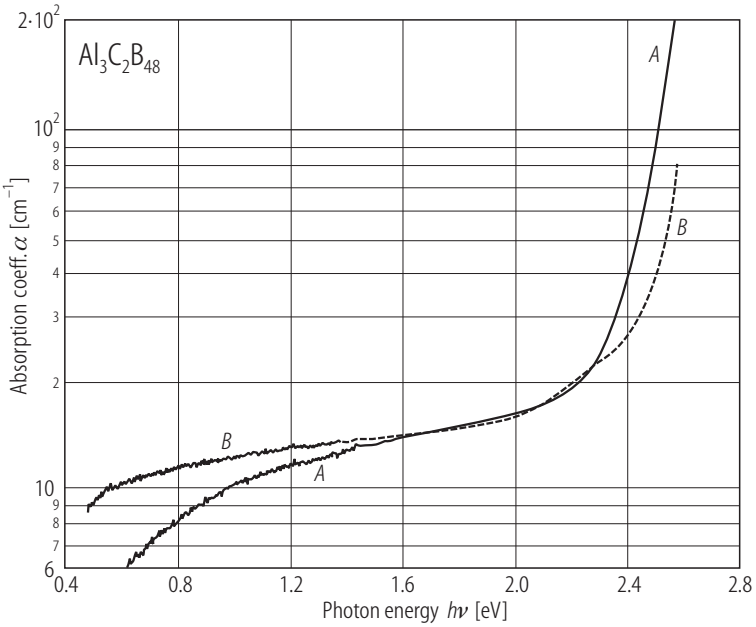

Fig. 5.

$Al_3C_2B_{48}$. Phonon spectra. Upper curve, IR transmission, lower curve, Raman intensity vs. wavenumber [98M].

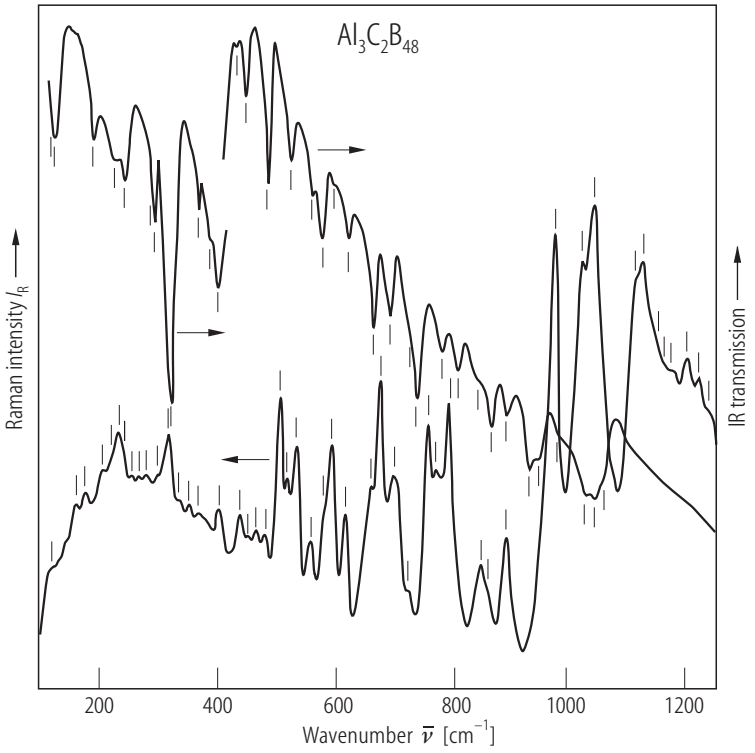

Fig. 6.

$Al_3C_2B_{48}$:Si. Phonon spectra of $Al_{1.5}Si_{1.5}C_2B_{48}$. Upper curve, IR transmission, lower curve, Raman intensity vs. wavenumber [98M].

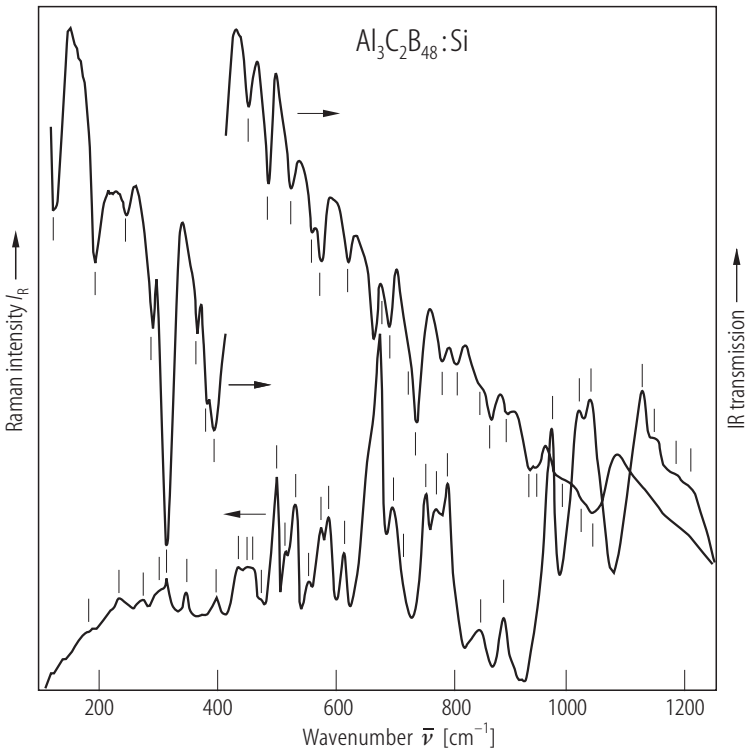

Fig. 7.

$Al_3C_2B_{48}$. Electrical conductivity; σT vs. reciprocal temperature [91K1].

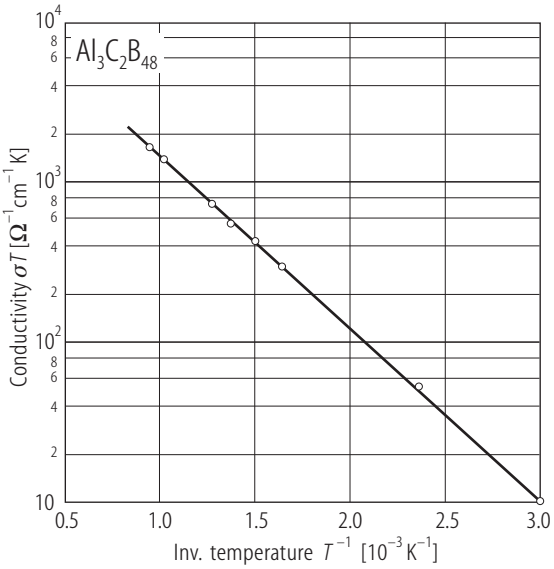

Fig. 8.

$Al_3C_2B_{48}$. Thermoelectric power *S* vs. *T* [91K1].

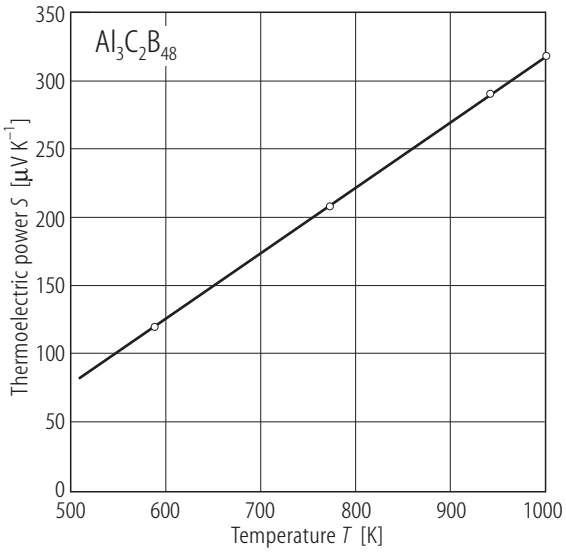

Fig. 9.

$Al_3C_2B_{48}$, $Al_8B_4C_7$. Effect of Fe-doping on the thermoelectric power; *S* vs. Fe content [91K1].

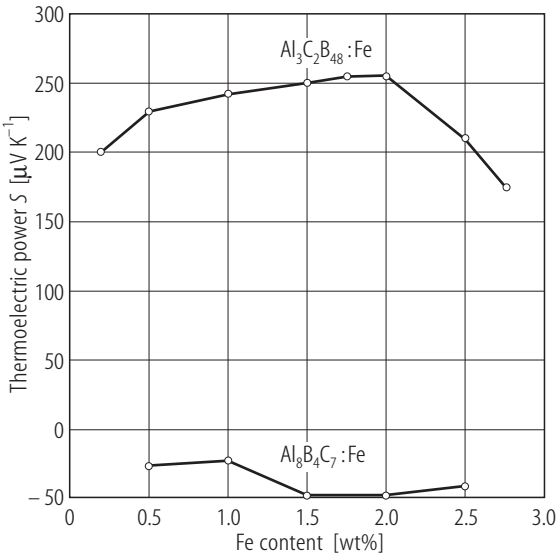

Fig. 10.

$Al_3C_2B_{48}$. DTA curves; upper curve: heating; lower curve: cooling [98M].

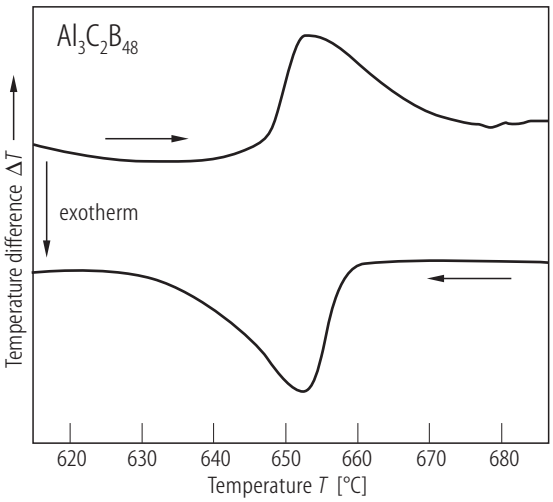

Fig. 11.

$Al_3C_2B_{48}$:Si. Vickers microhardness vs. atomic ratio Si/B [94K1].